COMMUNICATION

ChemFET Anion Sensor Based on MOF Nanoparticles

Douglas H. Banning,‡[a] Audrey M. Davenport,‡[a] Natalie M. Lakanen,[a] Jiawei Huang,[a] Carl K. Brozek,*[a] and Darren W. Johnson*[a]

[a] D. H Banning, A. M Davenport, N. M. Lakanen, J. Huang, C. K. Brozek, and D. W. Johnson
Department of Chemistry & Biochemistry and Materials Science Institute
University of Oregon
97403-1253 Eugene, OR, USA
E-mail: cbrozek@uoregon.edu; dwj@uoregon.edu

‡ Both authors contributed equally to this work

Abstract: Nanoparticles of metal-organic frameworks (nanoMOFs) possess the unusual combination of both internal and external surfaces. While internal surfaces have been the focus of fundamental and applications-based MOF studies, the chemistry of the external surfaces remains scarcely understood. Herein we report that specific ion interactions with nanoparticles of Cu(1,2,3-triazolate)$_2$ (Cu(TA)$_2$) resemble the Hofmeister behavior of proteins and the supramolecular chemistry of synthetic macromolecules. Inspired by these anion-selective interactions, we tested the performance of Cu(TA)$_2$ nanoparticles as chemical field effect transistor (ChemFET) anion sensors. Rather than size-based selectivity, the detection limits of the devices exhibit a Hofmeister trend, with the greatest sensitivity towards anions perchlorate, iodide, and nitrate. These results highlight the importance of the pore-based supramolecular interactions, rather than localized donor-acceptor pairs, in designing MOF-based technologies.

Metal-organic frameworks (MOFs) are an exciting area of materials chemistry with a wide range and continually expanding array of interesting properties[1–3] and applications that include gas capture,[4,5] remediation,[6,7] catalysis,[8,9] nanocrystal formation,[10,11] thin films,[12,13] and sensing.[13–17] Specifically in chemically-sensitive field effect transistor (ChemFET) sensing applications, MOFs have been most commonly used for gas detection.[14,18] ChemFETs are an electrochemical sensing tool that has previously been well-characterized in developing affinity profiles for host-guest interactions.[19–24,24–26] ChemFETs utilize host incorporation into a semipermeable membrane to provide a response specific to the functionalized membrane and the analyte of interest. In the cases of MOF evaluations via ChemFETs, a MOF-functionalized gate oxide is one of the more common methods of integrating MOFs into ChemFET-based sensor systems.[14,18] Despite the impressive sensitivity of MOF-based ChemFET sensors, little is known about the underlying guest-host chemical interactions between the analytes and MOFs. Additionally, deployment of these technologies at-scale will require facile fabrication of uniform MOF thin films or polymer-hybrids, as with chemical separation membranes or other recent MOF-based industrial technologies.[27] Whereas typical reports of MOF sensors employ bulk powder, nanoparticles (nanoMOFs) offer the ability to use solution processable techniques ranging from drop-casting and doctor-blading, to spin- and spray-coating.[28] Here, we report the design of nanoMOF-based ChemFET anion sensors based on chemical insight into the specific guest-host chemistry underlying the MOF-analyte interactions.

Scheme 1. Representation of a portion of the Cu(1,2,3-triazolate)$_2$ (Cu(TA)$_2$) pore aperture versus n-butyl bambus[6]uril, a previously-characterized anion receptor. Hydrogen atoms omitted for clarity.

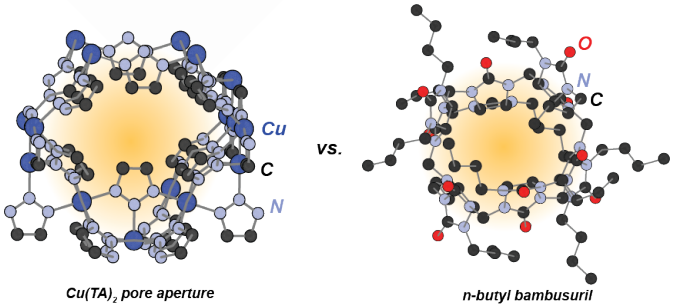

In search of MOFs with the potential for selective anion interactions, we identified Cu(1,2,3-triazolate)$_2$ as having a similar pore size (ca. 5-6 Å in diameter) and chemical environment to the well-known bambus[6]uril family of anion receptors.[24,25,29] Whereas most MOF pores exceed 10 Å, M(TA)$_2$ M = Mg, Cr, Mn, Fe, Co, Zn, Cd possess unusually small pores.[30,31] Previously, we demonstrated that such narrow pore apertures frustrate the ability of anions to intercalate into electrochemical thin films of M(TA)$_2$ M = Cr, Fe nanoparticles.[10,32] The oxidation of interior Fe sites anodically shifts ca. 1.5 V due to the additional anion desolvation and solvent reorganization in comparison to the charge compensation mechanism involving exterior Fe sites. The larger pore apertures of Cr(TA)$_2$ permitted redox intercalation of a range of anions, but where the associated redox potentials varied by hundreds of mV depending on the anion size.[33] This electrochemical behavior suggested that constricted pore environments of Cu(TA)$_2$ would display anion-specific interactions due to the close proximity of anions to the pore walls, especially for anions with similar diameters to the pores.

The synthesis of the Cu(TA)$_2$ followed previously published procedures for M(TA)$_2$, M = Co, Fe, Cr.[10] Briefly, Cu(NO$_3$)$_2$•H$_2$O was dissolved in anhydrous DMF to afford a 10 mM solution, to which was added 1,2,3-triazole with vigorous stirring. This mixture was heated at 120 °C for 2 h on a dry bath. Particles were collected by centrifugation, washed twice with fresh DMF and twice with fresh methanol, and desolvated under reduced

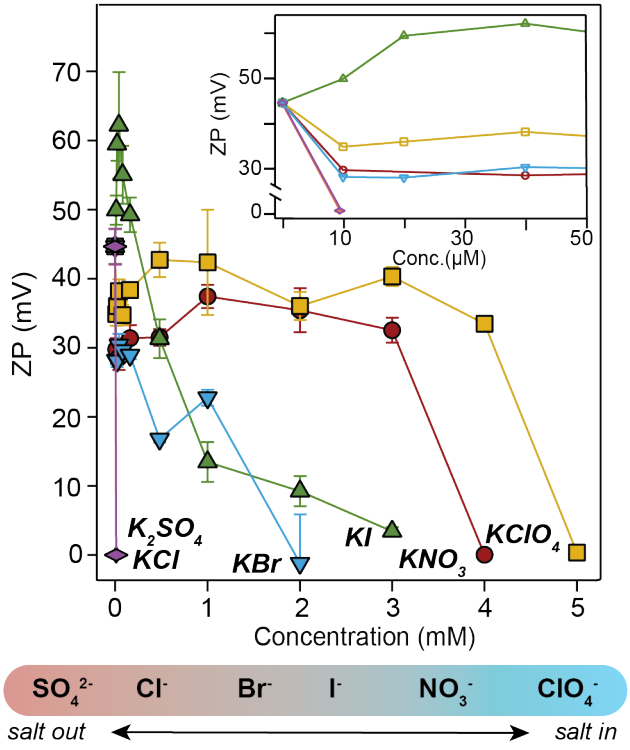

Figure 1. Zeta potentials of 30-nm $Cu(TA)_2$ colloidal nanoparticles suspended in DMF solutions. Electrolyte salts were added sequentially in increasing concentrations as indicated in mM. All measurements were recorded in triplicate. Solvation diameters were recorded simultaneously by dynamic light scattering and are included in the ESI. Anions are ordered based on the electrolyte concentrations required to reach the PZC, which conforms well to standard Hofmeister ordering of anions. Inset: Zeta potentials recorded at low electrolyte concentrations.

pressure via standard Schlenk techniques. Particle sizes and dispersities were measured by Scherrer analysis of PXRD patterns, dynamic light scattering (DLS), and scanning electron microscopy (SEM).

For microscopic insight into the interactions of $Cu(TA)_2$ nanoparticles with anions, zeta potentials and DLS sizes were recorded in tandem during the titration of potassium salts. Such measurements have been critical in understanding the surface chemistry of proteins and conventional, nonporous colloidal nanoparticles.[34,35] Salts that cause zeta potentials to reach 0 mV at lower concentrations interact more strongly with the nanoparticle surface, typically causing the particles or proteins to "salt out". Interestingly, in DMF $Cu(TA)_2$ particles have a remarkably high zeta potential which suggests not only excellent colloidal stability, but also the presence of open metal sites at the surface of the particles (Scheme 1). In general, 3 mg/mL 30-nm $Cu(TA)_2$ nanoparticles in DMF were treated with stock solutions of 10 μM and 100 μM of DMF solutions of each electrolyte using appropriate volumetric amounts to reach the desired electrolyte concentrations. Measurements were collected in triplicate. The resulting data are shown in Fig. 1. Although all salts eventually caused zeta potentials to reach a "point of zero charge" (PZC), only KI and KBr induced nanoparticle precipitation. Interestingly, the order of electrolyte concentrations required to reach the PZC resembles the ordering observed for proteins, now well-known as the Hofmeister series.[24,25,36] It is important to note that zeta potentials report on the "slipping plane" of a colloid, which, depending on the system, corresponds to the inner solvation shell or several nanometers from the nanoparticle surface. Therefore, these results suggest a considerable selectivity of anion interactions with the external surface of $Cu(TA)_2$ nanoparticles.

Given the structural similarity between the $Cu(TA)_2$ pores and the binding pockets of previously-characterized anion receptors, a plan was developed to follow previous electrochemical sensing methodology to characterize the "host"-like nature of the pores interacting with aqueous anion "guests." These previous studies involved the use of chemically sensitive field-effect transistors (ChemFETs) to evaluate the host-guest interaction of host receptors with anion guests. Since the applications of interest for previous projects involved aqueous anion affinity, they necessitated some approach tolerant of characterizing interactions between both hydrophobic hosts and aqueous guests. ChemFETs indeed demonstrated suitable bridging of this solubility gap.

ChemFETs are a useful tool that have been used in sensing applications to evaluate aqueous anion affinity of hydrophobic anion receptors.[22–25] Previous work evaluated various organic anion receptors for aqueous anion affinity trends.[24,25] A series of control sensors are also used to contrast with the receptor results, in order to analyze any deviations from the Hofmeister series in the anion affinity profiles caused by the receptors. These control sensors lack the MOF but still contain all of the other components of the ChemFET (polymer, ionophore/immobilized cation, plasticizer).

Related studies in ChemFET sensors using MOFs have investigated functionalizing the gate oxide surface of FETs with MOFs to provide chemical selectivity.[14,18] Our initial attempt at using $Cu(TA)_2$ to bias selectivity in ChemFET sensors followed

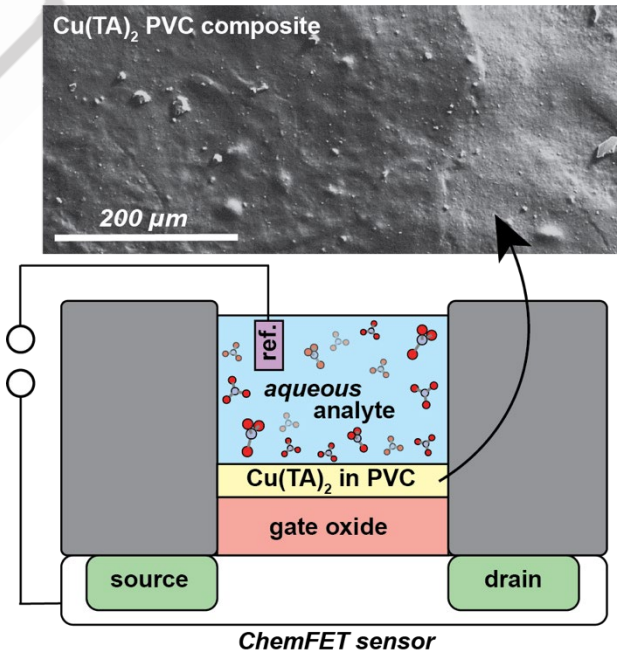

Figure 2. ChemFET sensor construction for MOF evaluation. Sensor depicted contains $Cu(TA)_2$ in the PVC membrane. Control sensors were identically constructed with PVC membrane, just without $Cu(TA)_2$ providing selectivity. An SEM image of the control is included the ESI.

these literature precedents. However, in this case all attempts at functionalizing the gate oxide surface with $Cu(TA)_2$ failed. Therefore, we pivoted to emulate aspects of previous studies by us and others that used organic anion receptors within ChemFET membranes to impart selectivity.[22–25] This well-established approach involves integration of receptors into a polyvinyl chloride (PVC)-based membrane to facilitate aqueous anion affinity evaluation.[22–25]

Another benefit of this approach is that integrating MOF particles into the ChemFET membrane facilitates the direct comparison of sensors with MOF-containing membrane to sensors containing a control membrane that lacks the MOF. These control sensors are created identically in all respects, with the exception of addition of any anion receptor, and therefore, these control receptors will simply respond to anions with Hofmeister trend selectivity. This facilitates creation of a control profile for comparison purposes that is unavailable to ChemFET evaluations with a functionalized gate oxide. Therefore, the detection limit of each anion with MOF-containing sensors was able to be compared to a corresponding "blank" run, further isolating the difference in response entirely to inclusion of the MOF. Thus, the host-guest interaction of the anion with the MOF accounts for the entire difference between control and MOF-containing sensor results.

Sensor evaluation was performed following previously published reports.[22–25] The MOF was incorporated into a ChemFET membrane dropcast solution for application to the FET. The MOF was incorporated as 1 wt% of the dropcast solution, with 2 wt% tetraoctylammonium nitrate (TOAN), 32 wt% *o*-nitrophenyl octyl ether (NPOE) plasticizer, and 65 wt% high molecular weight PVC. The sensors were then coated by drop-casting four 1.6 µL drops of the receptor onto the surface of the FETs. The drops were applied in thirty-minute intervals to allow for solvent removal. Following the completion of the dropcasting, the ChemFET sensors were then placed in a 60 °C oven overnight to ensure complete solvent removal. The sensors were then allowed to cool over another 24 hours before the evaluation began.

The evaluation comprised four identically constructed chemFET sensors with the $Cu(TA)_2$ incorporated into the PVC-based selective membrane (Figure 2). The four sensors were then run through a series of 12 solutions of increasing analyte concentration: 0.500 µM, 1.00 µM, 5.00 µM, 10.0 µM, 50.0 µM, 100 µM, 500 µM, 1.00 mM, 5.00 mM, 10.0 mM, 50.0 mM, and 0.100 M, with each containing a constant 50.0 mM piperazine-N,N′-bis-2-ethanesulfonic acid (PIPES) acting as a non-interfering buffer to ensure consistent ionic strength of the solution even at low analyte concentrations (this avoids a misleadingly low detection limit stemming from the low ionic strength of the low concentration solutions). A set of four sensors was run through the 12 series of analyte solutions in triplicate: from low concentration to high, then high to low, and then finally low to high, and the data averaged to provide the reported metrics. An anion affinity profile was evaluated for a series of seven common anions in the Hofmeister series to illuminate whether the $Cu(TA)_2$-containing sensors followed a Hofmeister-like trend or a size exclusion trend (Figure 3).[37]

The ChemFET sensor evaluation of $Cu(TA)_2$ indicated an affinity profile consistent with a Hofmeister trend rather than a size-based trend (Figure S10). Chaotropes (or more lipophilic anions) such as iodide, perchlorate, and nitrate produced low detection limits (µM), while kosmotropes (harder, more hydrophobic anions) such as sulfate and fluoride produced high detection limits (M). Ordering of the Hofmeister series follows the computational work of Page et al. based on linear charge density of each anion.[37] Therefore, in the context of ChemFET-based sensors, the affinity profile clearly does not follow the size trend first suggested by electrochemical measurements of the MOF nanocrystals in solution.[38] Interestingly, the evaluation of $Cu(TA)_2$ host-guest interactions with a series of anions paralleled the same Hofmeister trend found for organic anion receptors that featured a similar pore size to the MOF.[24,25] In effect, there appears to be a Hofmeister "cutoff" in sensor selectivity around bromide, where the sensor has quite strong selecitivity for anions more lipophilic than bromide (versus control ionophore-containing receptor) and on par with the best organic host containing ChemFET we have screened.[25] It is also important to note that the counter cation remained constant during these experiments to rule out any impact on the anion affinity profile: potassium was used as the counter cation for all anions evaluated.

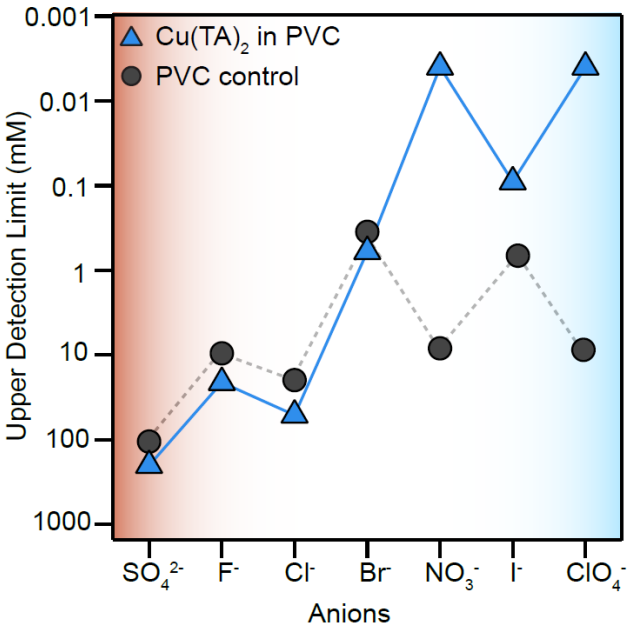

Figure 3. Anion affinity profile as evaluated via $Cu(TA)_2$-containing ChemFET sensors. Upper bounds for detection limits (based on error, see ESI Table S2) are presented on a log scale, with lower detection limits (better) located higher on the chart. Table S2 contains errors for each measurement. All counter cations are potassium to eliminate influence of cation on the anion affinity profile. Lines are used as a guide to the eye to distinguish between data sets.

In conclusion, we report an anion-dependent affinity of MOF nanoparticles that follows a Hofmeister trend of Lewis acid/base hard/soft theory rather than a simple size-exclusion mechanism. These results suggest that MOF pores—the alternating regions of hydrophobicity/hydrophilicity, polarizability, and nanoconfined topologies—resemble the supramolecular chemistry of proteins and macrocyclic ion receptors. Beyond anion sensing, these results provide design principles for gas sorption, catalysis, and other MOF applications involving guest-host chemistry. In addition to their practical utility, the ChemFET sensors are critical

to establishing this fundamental connection between MOF and macromolecular chemistry.

Supporting Information

The authors have cited additional references within the Supporting Information.[22–26,39]

Acknowledgments

We thank the NIH (R21-GM129590 to D. W. J.), the NSF Division of Materials Research (DMR-2114430 to C.K.B.), the NSF Research Experiences for Undergraduates scholarship to N.M.L. (CHE-1949900), and the University of Oregon for support of this research. C.K.B. gratefully acknowledges support from the Research Corporation for Science Advancement through the Cottrell Scholar Award. This work was also supported by the Bradshaw and Holzapfel Research Professorship in Transformational Science and Mathematics to D. W. J., and the Air Force Institute of Technology (D. H. B.).

Keywords: anion recognition • metal organic frameworks • ChemFET • sensors • Hofmeister

[1] J. R. Long, O. M. Yaghi, *Chem. Soc. Rev.* **2009**, *38*, 1213–1214.
[2] H. Furukawa, K. E. Cordova, M. O'Keeffe, O. M. Yaghi, *Science* **2013**, *341*, 1230444.
[3] H.-C. "Joe" Zhou, S. Kitagawa, *Chem. Soc. Rev.* **2014**, *43*, 5415–5418.
[4] M. Ding, R. W. Flaig, H.-L. Jiang, O. M. Yaghi, *Chem. Soc. Rev.* **2019**, *48*, 2783–2828.
[5] J.-R. Li, R. J. Kuppler, H.-C. Zhou, *Chem. Soc. Rev.* **2009**, *38*, 1477–1504.
[6] R. M. Rego, G. Kuriya, M. D. Kurkuri, M. Kigga, *J. Hazard. Mater.* **2021**, 123605.
[7] K. Ventura, R. A. Arrieta, M. Marcos-Hernández, V. Jabbari, C. D. Powell, R. Turley, A. W. Lounsbury, J. B. Zimmerman, J. Gardea-Torresdey, M. S. Wong, D. Villagrán, *Sci. Total Environ.* **2020**, 139213.
[8] J. Lee, O. K. Farha, J. Roberts, K. A. Scheidt, S. T. Nguyen, J. T. Hupp, *Chem. Soc. Rev.* **2009**, *38*, 1450–1459.
[9] J. Baek, B. Rungtaweevoranit, X. Pei, M. Park, S. C. Fakra, Y.-S. Liu, R. Matheu, S. A. Alshmimri, S. Alshehri, C. A. Trickett, G. A. Somorjai, O. M. Yaghi, *J. Am. Chem. Soc.* **2018**, *140*, 18208–18216.
[10] J. Huang, C. R. Marshall, K. Ojha, M. Shen, S. Golledge, K. Kadota, J. McKenzie, K. Fabrizio, J. B. Mitchell, F. Khaliq, A. M. Davenport, M. A. LeRoy, A. N. Mapile, T. T. Debela, L. P. Twight, C. H. Hendon, C. K. Brozek, *J. Am. Chem. Soc.* **2023**, *145*, 6257–6269.
[11] A. M. Spokoyny, D. Kim, A. Sumrein, C. A. Mirkin, *Chem. Soc. Rev.* **2009**, *38*, 1218–1227.
[12] D. Zacher, O. Shekhah, C. Wöll, R. A. Fischer, *Chem. Soc. Rev.* **2009**, 1418–1429.
[13] O. Shekhah, J. Liu, R. A. Fischer, C. Wöll, *Chem. Soc. Rev.* **2011**, *40*, 1081–1106.
[14] N. Ingle, P. Sayyad, G. Bodkhe, M. Mahadik, T. AL-Gahouari, S. Shirsat, M. D. Shirsat, *Appl. Phys. A* **2020**, *126*, 723.
[15] M. Ko, L. Mendecki, A. M. Eagleton, C. G. Durbin, R. M. Stolz, Z. Meng, K. A. Mirica, *J. Am. Chem. Soc.* **n.d.**, *27*, 11717–11733.
[16] A. Aykanat, Z. Meng, R. M. Stolz, C. T. Morrell, K. A. Mirica, *Angew. Chem., Int. Ed.* **2022**, *134*, e202113665.
[17] M. G. Campbell, S. F. Liu, T. M. Swager, M. Dincă, *J. Am. Chem. Soc.* **2015**, *137*, 13780–13783.
[18] M. S. More, G. A. Bodkhe, F. Singh, Babasaheb. N. Dole, M.-L. Tsai, T. Hianik, M. D. Shirsat, *Synth. Met.* **2023**, *296*, 117357.
[19] D. N. Reinhoudt, *Sens. Actuators, B* **1995**, *24*, 197–200.
[20] P. L. H. M. Cobben, R. J. M. Egberink, J. G. Bomer, P. Bergveld, W. Verboom, D. N. Reinhoudt, *J. Am. Chem. Soc.* **1992**, *114*, 10573–10582.
[21] M. M. G. Antonisse, D. N. Reinhoudt, *Electroanalysis* **1999**, *11*, 1035–1048.
[22] G. M. Kuhl, D. T. Seidenkranz, M. D. Pluth, D. W. Johnson, S. A. Fontenot, *Sens. Bio-Sens. Res.* **2021**, *31*, 100397.
[23] T. J. Sherbow, G. M. Kuhl, G. A. Lindquist, J. D. Levine, M. D. Pluth, D. W. Johnson, S. A. Fontenot, *Sens. Bio-Sens. Res.* **2021**, *31*, 100394.
[24] G. M. Kuhl, D. H. Banning, H. A. Fargher, W. A. Davis, M. Howell, L. N. Zakharov, M. D. Pluth, D. W. Johnson, *Chem. Sci.* **2023**, *14*, 10273–10279.
[25] D. H. Banning, G. M. Kuhl, M. M. Howell, D. W. Johnson, *Org. Biomol. Chem.* **2024**, *22*, 269–273.
[26] D. H. Banning, G. M. Kuhl, S. A. Fontenot, D. W. Johnson, *Supramol. Chem.* **2024**, *Accepted Manuscript*, DOI 10.1080/10610278.2024.2353565.
[27] W. S. Chi, B. J. Sundell, K. Zhang, D. J. Harrigan, S. C. Hayden, Z. P. Smith, *ChemSusChem* **2019**, *12*, 2355–2360.
[28] K. Fabrizio, E. L. Gormley, A. M. Davenport, C. H. Hendon, C. K. Brozek, *Chem. Sci.* **2023**, *14*, 8946–8955.
[29] M. D. Hanwell, D. E. Curtis, D. C. Lonie, T. Vandermeersch, E. Zurek, G. R. Hutchison, *J. Cheminf.* **2012**, *4*, 17.
[30] F. Gándara, F. J. Uribe-Romo, D. K. Britt, H. Furukawa, L. Lei, R. Cheng, X. Duan, M. O'Keeffe, O. M. Yaghi, *Chem. - Eur. J.* **2012**, *18*, 10595–10601.
[31] J. G. Park, M. L. Aubrey, J. Oktawiec, K. Chakarawet, L. E. Darago, F. Grandjean, G. J. Long, J. R. Long, *J. Am. Chem. Soc.* **2018**, *140*, 8526–8534.
[32] C. R. Marshall, J. P. Dvorak, L. P. Twight, L. Chen, K. Kadota, A. B. Andreeva, A. E. Overland, T. Ericson, A. F. Cozzolino, C. K. Brozek, *J. Am. Chem. Soc.* **2022**, *144*, 5784–5794.
[33] J. Huang, K. Heffernan, T. Devela, C. Marshall, A. M. Davenport, J. McKenzie, M. Shen, S. Hou, J. Mitchell, K. Ojha, C. H. Hendon, C. K. Brozek, *J. Am. Chem. Soc.* **in press**, DOI 10.1021/jacs.4c06669.
[34] S. Salgın, U. Salgın, S. Bahadır, *Int. J. Electrochem. Sci.* **2012**, *7*, 12404–12414.
[35] A. Salis, M. Boström, L. Medda, F. Cugia, B. Barse, D. F. Parsons, B. W. Ninham, M. Monduzzi, *Langmuir* **2011**, *27*, 11597–11604.
[36] W. Yao, K. Wang, A. Wu, W. F. Reed, B. C. Gibb, *Chem. Sci.* **2021**, *12*, 320–330.
[37] K. P. Gregory, E. J. Wanless, G. B. Webber, V. S. J. Craig, A. J. Page, *Chem. Sci.* **2021**, *12*, 15007–15015.
[38] Y. Marcus, *J. Chem. Soc., Faraday Trans.* **1991**, *87*, 2995–2999.
[39] M. Grzywa, D. Denysenko, J. Hanss, E.-W. Scheidt, W. Scherer, M. Weil, D. Volkmer, *Dalton Trans.* **n.d.**, *41*, 4239.

Entry for the Table of Contents

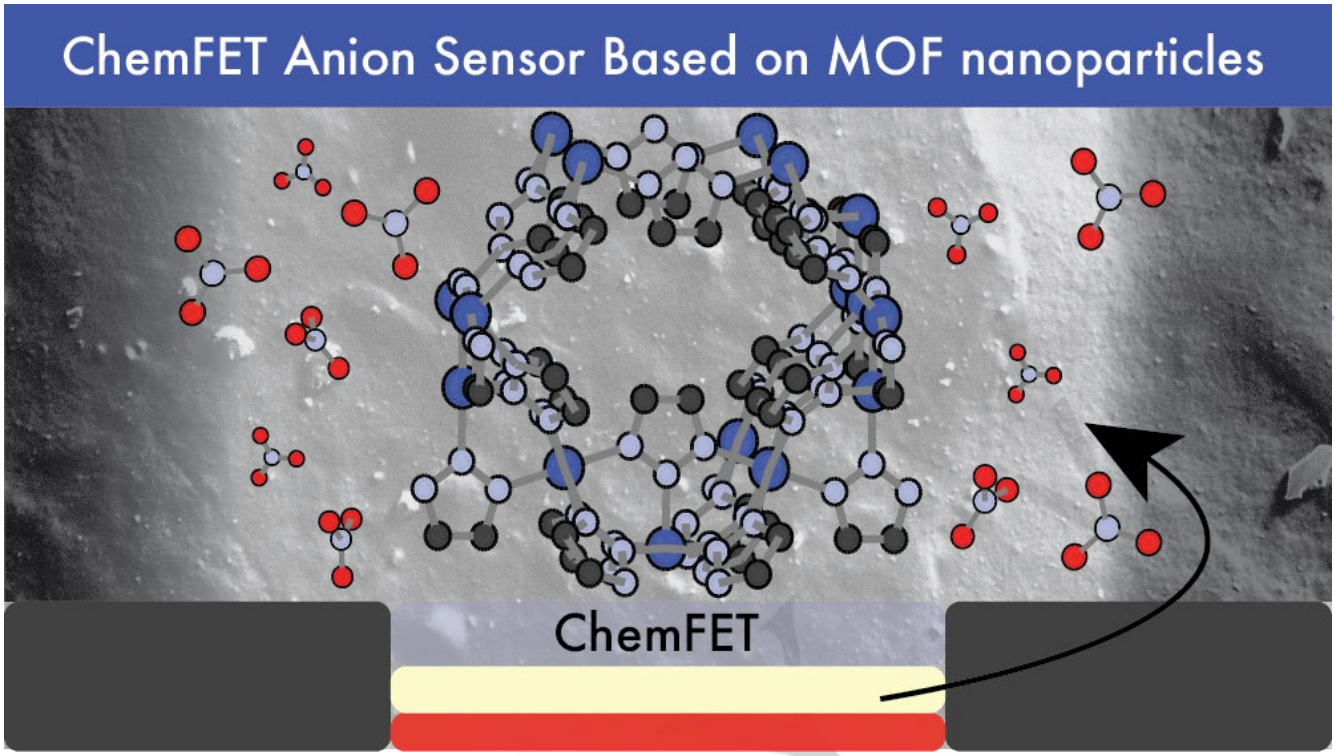

Nanoparticles of metal-organic frameworks (nanoMOFs) possess internal and external surface features that mimic the shapes and binding capacities of proteins and supramolecular hosts. A Cu(1,2,3-triazolate)$_2$ nanoMOF presents external surface features in a ChemFET anion sensor to provide Hofmeister-like anion binding selectivity rivalling that of conventional supramolecular approaches.